

A low $[Ca^{2+}]_i$ -induced enhancement of cAMP-activated ciliary beating by PDE1A inhibition in mouse airway cilia

Haruka Kogiso¹ · Shigekuni Hosogi^{1,2} · Yukiko Ikeuchi¹ · Saori Tanaka³ · Chikao Shimamoto³ · Hitoshi Matsumura³ · Takashi Nakano⁴ · Koh-ichi Sano⁴ · Toshio Inui^{1,2,5} · Yoshinori Marunaka^{1,2,6} · Takashi Nakahari^{1,2,6}

Received: 14 February 2017 / Revised: 19 April 2017 / Accepted: 24 April 2017 / Published online: 5 May 2017
© Springer-Verlag Berlin Heidelberg 2017

Abstract This study demonstrated that PDE1 (phosphodiesterase 1) existing in the ciliary beat frequency (CBF)-regulating metabolon regulates CBF in procaterol-stimulated lung airway ciliary cells of mouse. Procaterol (an β_2 -agonist) increased the ciliary bend angle (CBA) and CBF via cAMP accumulation in the ciliary cells of mice: interestingly, the time course of CBF increase was slower than that of CBA increase. However, IBMX (3-isobutyl-1-methylxanthine, an inhibitor of PDE) increased CBA and CBF in an identical time course. Lowering an intracellular Ca^{2+} concentration ($[Ca^{2+}]_i$) caused by switching to an EGTA-containing Ca^{2+} -free solution from normal one elevated the procaterol-induced increasing rate of CBF. These observations suggest that Ca^{2+} -dependent PDE1 controls cAMP-stimulated CBF increase. Either application of 8MmIBMX (8-methoxymethyl-IBMX, a selective PDE1 inhibitor), BAPTA-AM (an intracellular Ca^{2+} chelator), or calmidazolium (an inhibitor of calmodulin) alone increased CBA and CBF in the lung airway ciliary cells and

increased cAMP contents in the isolated lung cells, and like IBMX, each application of the compound made the time courses of CBA and CBF increase stimulated by procaterol identical. The immunoelectron microscopic examinations revealed that PDE1A exists in the space between the nine doublet tubules ring and plasma membrane in the lung airway cilium, where the outer dynein arm (a molecular motor regulating CBF) functions. In conclusion, PDE1A is a key factor slowing the time course of the procaterol-induced increase in CBF via degradation of cAMP in the CBF-regulating metabolon of the mouse lung airway cilia.

Keywords Airway cilia · PDE1 · Ciliary beating · Dynein · Procaterol

Introduction

Mucociliary transport, which is a host-defense mechanism of the lung, consists of the mucous layer and the beating cilia lining on the airway surface. The surface mucous layer entraps inhaled small particles, such as cellular debris, dusts, chemicals, bacteria, and viruses, and the beating cilia transport the mucous layer with entrapped small particles to the oropharynx [1, 21, 28]. Thus, the mucociliary transport is compared to a belt conveyor system removing inhaled particles from the airway [7], in which the beating cilia are the engine. The activation of ciliary beating is assessed by two parameters, i.e., the ciliary bend angle (CBA, an index of ciliary bend amplitude) and ciliary beat frequency (CBF) [15].

The previous study demonstrated that procaterol, a β_2 -agonist, increases both CBA and CBF mediated via cAMP accumulation in mouse lung airway ciliary cells [15]. However, procaterol increased CBF slower than CBA in the time course and was more effective to CBA than CBF [15]. These

✉ Takashi Nakahari
nakahari@koto.kpu-m.ac.jp

¹ Department of Molecular Cell Physiology, Graduate School of Medical Science, Kyoto Prefectural University of Medicine, Kyoto, Japan
² Bio-Ionomics, Graduate School of Medical Science, Kyoto Prefectural University of Medicine, Kyoto, Japan
³ Laboratory of Pharmacotherapy, Osaka University of Pharmaceutical Sciences, Takatsuki, Japan
⁴ Department of Microbiology and Infection Control, Osaka Medical College, Takatsuki, Japan
⁵ Saisei Mirai Clinics, Moriguchi, Japan
⁶ Japan Institute for Food Education and Health, St Agnes' University, Kyoto, Japan

observations suggest that the CBF-regulating pathway is distinct from the CBA-regulating pathway in lung airway ciliary cells.

A cilium is composed of the axoneme (nine doublet microtubules (A- and B-tubules) in a ring surrounding a central pair of microtubules) [1, 21, 28]. Axonemal beating is driven by the two functionally distinct dyneins (molecular motors), namely, the inner dynein arm (IDA) attached to the inner side of the A tubules and the outer dynein arm (ODA) attached to the outer side of the A tubules [1, 3, 4, 10, 21, 28]. The IDAs change the waveform, including CBA, whereas the ODAs change the frequency (CBF) [1, 3, 4, 6, 11, 28, 29]. One possible explanation for the slower CBF increase during procaterol stimulation is that cAMP accumulation in the metabolon regulating ODA may be slower than that regulating IDA.

On the other hand, we examined the effects of an EGTA-containing Ca^{2+} -free solution (EGTA solution) on CBA and CBF increase stimulated by procaterol in the lung airway ciliary cells. Incubation in an EGTA solution did not induce any change in the basal CBF and CBA [15], while the rate of procaterol-stimulated CBF increase is higher in the EGTA solution than in the control solution. Moreover, IBMX (3-isobutyl-1-methylxanthine, a nonspecific inhibitor of PDE), unlike procaterol, increased both CBA and CBF in an identical time course. Based on these observations, the Ca^{2+} -dependent PDE1 appears to control CBF by regulating cAMP accumulation in the CBF-regulating metabolon. The aim of this study is to confirm PDE1 regulation of CBF during procaterol stimulation in the mouse lung airway ciliary cells.

Materials and methods

Solution and chemicals The control solution was composed of 121 mM NaCl, 4.5 mM KCl, 25 mM NaHCO_3 , 1 mM MgCl_2 , 1.5 mM CaCl_2 , 5 mM NaHEPES, 5 mM HEPES, and 5 mM glucose. To prepare the nominally Ca^{2+} -free solution, CaCl_2 (1.5 mM) was removed from the control solution and to prepare the EGTA-containing Ca^{2+} -free solution (EGTA solution), EGTA (1 mM) was added in the nominally Ca^{2+} -free solution. The pH of the solutions was adjusted to 7.4 by adding 1 M HCl or 1 M NaOH. All solutions were aerated with a gas mixture (95% O_2 and 5% CO_2) at 37 °C. The procaterol was a generous gift from Otsuka Pharmaceutical Co., Ltd. (Tokyo, Japan), and the concentration used was 1 nM throughout the experiments. 3-Isobutyl-1-methylxanthine (IBMX), 8-Br-cAMP (a nonhydrolyzable analogue of cAMP), heparin, elastase, and bovine serum albumin (BSA) were purchased from Wako Pure Chemical Industries, Ltd. (Osaka, Japan), BAPTA-AM and fluo4-AM were from Dojindo Laboratories (Kumamoto, Japan), calmidazolium and PKI 14-22 amide (PKI-A) were from

Tocris (Bristol, UK), 8-methoxymethyl-IBMX (8MmIBMX, a selective inhibitor of PDE1) was from Calbiochem (Darmstadt, Germany), and DNase I and dimethyl sulfoxide (DMSO) were from Sigma Chemical Co. (St Louis, MO, USA). All reagents were dissolved in DMSO or water as appropriate and prepared to their final concentrations immediately before the experiments. The DMSO concentration did not exceed 0.1%, and DMSO at this concentration has no effect on cellular events, such as changes in cell volume, $[\text{Ca}^{2+}]_i$ and intracellular pH including CBA and CBF [12, 15, 19, 23, 25].

Cell preparations Female mice (C57BL/6J, 5 weeks of age) were purchased from Shimizu experimental animals (Kyoto, Japan) and fed standard pellet food and water ad libitum. The lung epithelial cells, including airway ciliary cells, were isolated from the lungs as previously described [12, 15, 23]. The mice were first anesthetized and heparinized by an intraperitoneal injection of pentobarbital sodium (70 mg/kg) plus heparin (1000 units/kg) for 15 min and then, sacrificed by a high-dose pentobarbital sodium (100 mg/kg, ip). After the sacrifice, the lungs were cleared of blood by perfusion via the pulmonary artery using a nominally Ca^{2+} -free solution containing heparin (20 units/ml), and the lungs together with the trachea and heart were removed from the mouse en bloc. The procedure for cell isolation from the lungs has already been described in details elsewhere [12, 15, 23]. Briefly, a nominally Ca^{2+} -free solution was instilled into the lung cavity via the tracheal cannula (0.5 ml) and then, immediately removed. This procedure was repeated three times. The third instillation was retained in the lung cavity for 5 min, and the lung cavity was then washed five times with the control solution via the tracheal cannula. Finally, the control solution containing elastase (0.2 mg/ml) and DNase I (0.02 mg/ml) was instilled into the lung cavity via tracheal cannula and the lungs were incubated for 40 min at 37 °C. After this treatment, the lungs were minced by fine forceps in the control solution containing DNase I (0.02 mg/ml) and BSA (5%), and to isolate cells from undigested tissues, the minced tissue was filtered through a nylon mesh (a sieve having 300 μm openings). The isolated cells were washed three times with centrifugation (160 \times g for 5 min) and then re-suspended in the control solution at 4 °C. The cells were used for experiments within 5 h after the isolation. The procedures and protocols for the experiments were approved by the Committee for Animal Research of Kyoto Prefectural University of Medicine.

CBA and CBF measurements The cells were placed on a coverslip precoated with Cell-Tak (Becton Dickinson Labware, Bedford, MA, USA). The coverslips with cells were set in a microperfusion chamber (20 μl) that was mounted on an inverted light microscope (T-2000, NIKON, Tokyo, Japan) connected to a high-speed camera (FASTCAM-1024PCI,

Photron Ltd., Tokyo, Japan). The stage of the microscope was heated to 37 °C, because the CBF is temperature-dependent [7]. The chamber was perfused with the control solution aerated with a gas mixture (95% O₂ and 5% CO₂ at 37 °C) at a constant rate (300 µl/min). The ciliary cells were distinguished from other lung epithelial cells by their beating cilia. The ciliary cells accounted for around 10–20% of isolated lung cells. For the CBA and CBF measurements, video images were recorded for 2 s at 500 fps. Before the start of experiments, the cells were perfused with the control solution for 5 min and then with test solutions containing various drugs. After the experiments, CBA and CBF were measured using an image analysis program (DippMotion 2D, DITECT, Tokyo, Japan) [15]. To measure CBF, we superimposed a line on the video-image of the beating cilia, and the image analysis program reported any change in the light intensity on the line for 2 s. We measured CBF by counting the peaks on these traces. To measure CBA, two frame images in a cycle of ciliary beating were selected, one image showing a cilium in the end position of the effective stroke and the other showing the cilium in the start position of the effective stroke. The angle between the two positions was measured using an image analysis program (DippMotion 2D). The measured angle (CBA) was used as an index of ciliary bend amplitude [15]. The CBA and CBF ratios (CBA_{*t*}/CBA_{*0*} and CBF_{*t*}/CBF_{*0*}: normalized values of CBA and CBF) were calculated to make comparisons across the experiments. Five CBFs or CBAs measured for 5 min during control perfusion (1- or 2-min interval) were averaged and the averaged value was used as CBF_{*0*} or CBA_{*0*}. The subscripts “0” and “*t*” indicate the time from the start of experiments. Each experiment was carried out using 6–10 coverslips with cells obtained from three to five animals. For each coverslip, we selected a visual field with 1–2 cells or a cell-block and measured their CBAs or CBFs. The ratios of CBA and CBF were calculated by averaging values obtained from three to six cells (“*n*” shows the number of cells).

To avoid the operator bias, the blinded experiments were carried out in the control experiments (Fig. 1), the EGTA experiments (Fig. 1), and the 8MmIBMX experiments (Fig. 3) [24]. Prior to procaterol stimulation, the cells were perfused with a blinded solution, which is the control solution, the EGTA solution, or the 8MmIBMX-containing control solution, and then, they were stimulated with procaterol.

Measurement of cAMP contents The isolated lung cells were incubated in test solutions for 15 min at 37 °C. The test solution contains DMSO (vehicle control), calmidazolium (25 µM), 8MmIBMX (40 µM), IBMX (100 µM), or procaterol (1 nM) plus IBMX (100 µM) in the control solution. To decrease the [Ca²⁺]_{*i*}, the nominally Ca²⁺-free solution containing EGTA (1 mM) or BAPTA-AM (50 µM) was used. For the procaterol stimulation, two stimulation periods, 3 and

15 min, were used. After the experiments, the cells were immediately frozen by the liquid nitrogen and stored at –80 °C until the cAMP measurements. The contents of protein and cAMP in the cells were measured using a Pierce BCA Protein Assay kit (Thermo Fisher Scientific K.K, Yokohama, Japan) and a cAMP EIA kit (Cayman Chemical, Ann Arbor, MI, USA), respectively. The cAMP contents were expressed as micromoles/gram protein.

Measurement of the [Ca²⁺]_{*i*} The intracellular Ca²⁺ concentration ([Ca²⁺]_{*i*}) was measured using fluo 4 fluorescence. The isolated ciliary cells were incubated with 2.5 µM fluo4-AM (fluo4-acetoxymethyl ester) for 30 min at 37 °C. The fluo 4 fluorescence was measured using a confocal laser scanning microscope (model LSM 510META, Carl Zeiss, Jena, Germany). The fluo 4 was excited at 488 nm and the emission was 510 nm. The fluo 4 fluorescence ratio (*F_t/F₀*) was calculated. The subscripts *0* or *t* indicate the time from the start of experiments, respectively.

Western blot analysis Western blottings detecting PDE1A, PDE1B, and PDE1C were carried out using the isolated lung cells. The procedures for protein extraction and western blotting have already been described in the previous reports [19, 25]. The antibodies used were AP00651SU-S (Acris Antibodies, Germany) and ab14599 (Abcam plc, Cambridge, UK) against PDE1A, AP53233PU-N (Acris Antibodies, Germany) against PDE1B, and AP07024PU-N (Acris Antibodies, Germany) against PDE1C. The protein band was visualized by an enhanced chemiluminescence reagent (WSE-712 EzWestLumi plus, ATTO CORPORATION, Tokyo, Japan) and captured by a Lumino-image analyzer (LAS 3000; Fuji Film, Tokyo, Japan).

Immunofluorescence and immunoelectron microscopic examination For the electron microscopic examinations, the lungs were cleared of blood by perfusion via the pulmonary artery using a nominally Ca²⁺-free solution. Following the perfusion, glutaraldehyde (1%) in 0.15 M phosphate-buffered saline (PBS, pH 7.2) was infused into the lung cavity via tracheal cannula, and the lungs were removed from the trachea and further fixed with 1% glutaraldehyde in 0.15 M PBS at 4 °C for 1 h. The fixed lungs were washed five times with PBS and dehydrated in serially graded ethanol. The samples were then embedded in Lowicryl K4M resin (Electron Microscopy Science, PA, USA). Polymerization was allowed to occur in an ultraviolet irradiator (Dosaka EM, Kyoto, Japan) at –30 °C for 2 days and then at room temperature for 2 days. Ultrathin sections were prepared using a Porter Blum ultramicrotome (Sorvall MT-5000, Du Pont, CT, USA) and mounted on a 300-mesh nickel grid supported by a carbon-coated collodion film. Some samples were doubly fixed with 2% glutaraldehyde and 1% osmium tetroxide,

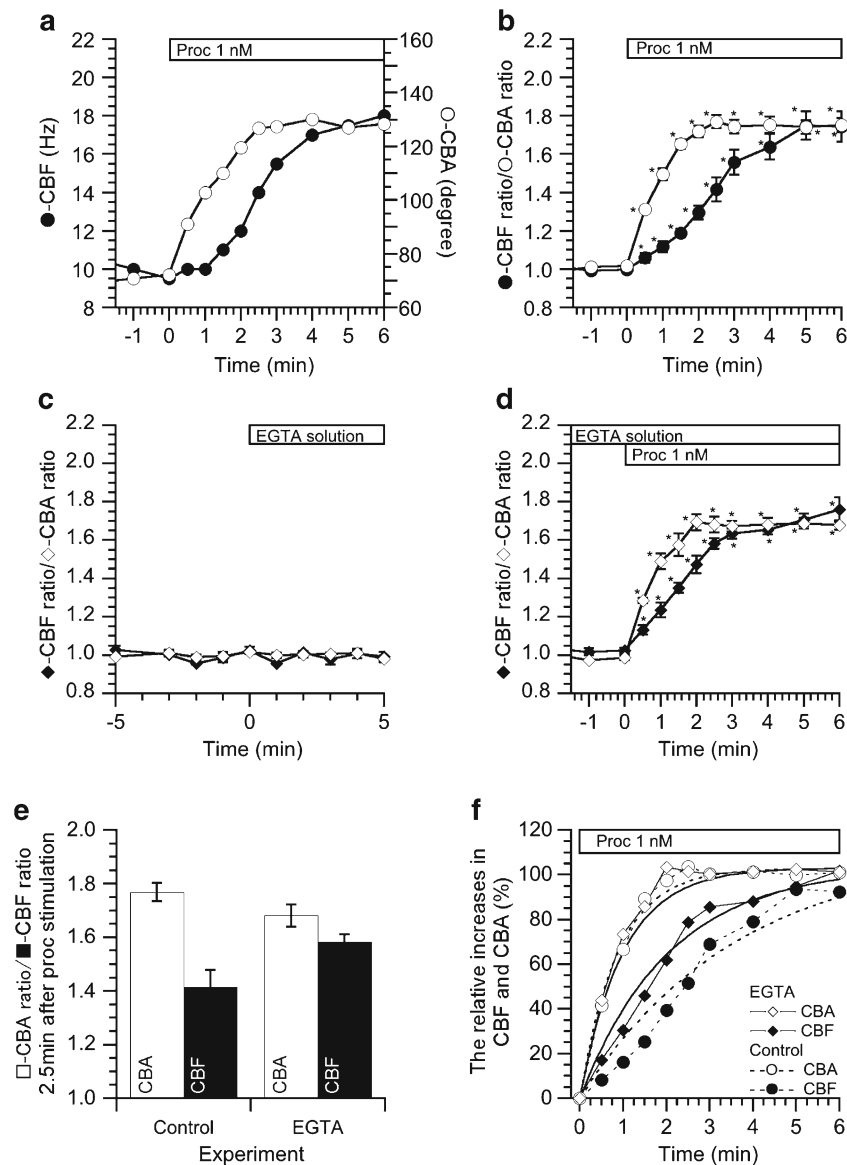


Fig. 1 Effects of 1 nM procaterol on CBA and CBF in airway ciliary cells. **a** A typical case showing CBA- and CBF increase in response to 1 nM procaterol. Stimulation with procaterol initially increased CBA and then CBF. CBA and CBF reached plateaus within 2.5 and 5 min from the start of procaterol stimulation, respectively. The time course of CBF increase was slower than that of CBA increase. CBA increased from 72° to 127° and CBF increased from 9.5 to 17.5 Hz. **b** Changes in the ratios of CBA and CBF (normalized values of CBA and CBF to the prestimulation values). Procaterol (1 nM) immediately increased CBA and then CBF. The CBA reached a plateau within 2 min (1.72 ± 0.03 , $n = 6$), whereas the CBF reached a plateau within 5 min (1.75 ± 0.07 , $n = 6$). **c** Effects of EGTA containing Ca^{2+} -free solutions (EGTA solution) on CBA and CBF in airway ciliary cells. In unstimulated airway ciliary cells, the switch to the EGTA solution did not induce any change in CBA and CBF. **d** Effects of EGTA solution on procaterol-stimulated CBA and CBF increase in airway ciliary cells. In the EGTA solution, procaterol increased CBA and CBF. But the CBF increase was accelerated by the EGTA solution. **e** Comparison of the ratios of CBA and CBF at 2.5 min

from the start of procaterol stimulation between control and EGTA experiments. The ratios of CBA and CBF stimulated by procaterol in the control solution were plotted from the **b** and those in the EGTA solution were plotted from the **d**. **f** The relative increase ratios of CBA and CBF in the first 6 min from the start of procaterol stimulation. The rate of CBA increase stimulated by procaterol in the EGTA solution was similar to that in the control solution, but the rate of CBF increase stimulated by procaterol in the EGTA solution was higher than that in the control solution. To compare the rate of CBA and CBF increase, the procaterol-stimulated CBA and CBF increase was fitted to an exponential curve ($= a \cdot [1 - \exp(-t/\tau)]$). The fitted curves were shown in the *solid lines* (EGTA solution experiments) and the *dotted lines* (control solution experiments). The τ for CBA increase in the EGTA solution was not different from that in the control solution, but the τ for CBF increase was smaller in the EGTA solution than in the control solution. Thus, the EGTA solution increased the rate of procaterol-stimulated CBF increase. The *asterisk signs* indicate significantly different from the values of CBA and CBF before procaterol stimulation ($p < 0.05$)

embedded in epoxy resin, and processed according to the routine procedure for electron microscopy [18, 20]. Ultrathin

sections on the grid were treated with 5% normal goat serum in PBS to inhibit nonspecific reactions. The sections were then

incubated with diluted rabbit antibody ($\times 5$) against PDE1A (AP00651SU-S, Acris Antibodies, Germany), PDE1B (AP53233PU-N, Acris Antibodies, Germany), or PDE1C (AP07024PU-N, Acris Antibodies, Germany) at 37 °C for 2 h and washed three times in PBS. The sections were allowed to react with 5-nm colloidal gold-labeled anti-rabbit IgG goat serum (EY Laboratories, CA, USA) at room temperature for 60 min and then washed three times. The immunostained sections were fixed with 1% glutaraldehyde in PBS and then washed three times in distilled water. Finally, the sections were stained with a mixture of 0.01% (*w/v*) ruthenium red and 0.5% (*w/v*) osmium tetroxide in PBS for 10 min prior to being stained with 4% (*w/v*) uranyl-acetate aqueous solution and examined under electron microscopes (H-7650, Hitachi Hi-tech, Tokyo, Japan) [18, 20].

The immunofluorescence images of the isolated ciliary cells were also observed using a confocal laser microscope (model LSM 510META, Carl Zeiss, Jena, Germany). The isolated lung cells attached on the coverslip were fixed in 4% paraformaldehyde for 30 min, dried, and then, they were permeabilized by 0.1% saponin (Nacalai tesque, Kyoto, Japan). For the immunofluorescence staining, the samples were incubated with an anti-PDE1A antibody (ab14599, Abcam plc, Cambridge, UK), PDE1B (AP53233PU-N, Acris Antibodies, Germany), an anti-PDE1C antibodies (AP07024PU-N, Acris Antibodies, Germany), or an anti-acetylated tubulin antibody (T6793, Sigma Chemical Co, MO, USA) for 12 h at 4 °C. After this incubation, the samples were incubated with the secondary antibodies for 2 h. The secondary antibody with Alexa Fluor 488 (1:500; Invitrogen, Carlsbad, CA, USA) or with Alexa Fluor 546 (1:500; Invitrogen, Carlsbad, CA, USA) was used for acetylated tubulin or for PDE1 subtypes (A, B, and C), respectively. The samples on the coverslip were enclosed with VECTASHIELD HardSet Mounting Medium with DAPI (Vector, Burlingame, CA, USA). Since AP00651SU-S (the anti-PDE1A antibody from Acris Antibodies, Germany) is not available in Japan after the experiments of immunoelectron microscopy, ab14599 (the anti-PDE1A antibody from Abcam plc, Cambridge, UK) was used for the immune-fluorescence chemistry experiments.

Statistical analysis Data are expressed as the means \pm standard error (SEM). Statistical significance between means was assessed by analysis of variance (ANOVA) or Student's *t* test, as appropriate. Differences were considered significant at $p < 0.05$. The statistical significances are shown in the figures.

Results

Effects of 1 nM procaterol on CBA and CBF Procaterol increased CBA and CBF in the lung airway ciliary cells. Figure 1a shows a typical case of CBA and CBF increase

stimulated by procaterol. In the unstimulated lung airway ciliary cells, CBA was 68°–72° and CBF was 9.5–10.5 Hz. Stimulation with procaterol immediately increased CBA to 127° within 2.5 min and gradually increased CBF to 18 Hz within 6 min. CBA and CBF 6 min after the procaterol addition were 128° and 18 Hz, respectively. Figure 1b shows increases in the ratios of CBA and CBF during procaterol stimulation, values of which are normalized to the basal condition. The CBA ratio reached a plateau within 2 min from the start of procaterol stimulation (CBA ratios at 2 and 5 min were 1.72 ± 0.03 ($n = 6$) and 1.74 ± 0.03 , respectively), whereas the CBF ratio reached a plateau approximately 5 min (CBF ratios at 2 and 5 min were 1.30 ± 0.04 ($n = 6$) and 1.75 ± 0.07 , respectively). Thus, the time course of CBF increase was slower than that of CBA increase.

The previous study demonstrated that procaterol increases CBA and CBA mediated via cAMP accumulation and not via $[Ca^{2+}]_i$ [15]. We examined the effects of a low $[Ca^{2+}]_i$ on the procaterol-induced increases in CBA and CBF. To decrease the $[Ca^{2+}]_i$, we used the EGTA solution. The switch to the EGTA solution from the Ca^{2+} -containing control solution did not induce any change in CBA and CBF (Fig. 1c) under the basal condition (without procaterol application). The further addition of procaterol immediately increased CBA and then CBF. However, the time course of CBF increase in the EGTA solution (closed diamond in Fig. 1d) was faster than that in the control solution (closed circles in Fig. 1b). In the EGTA solution, the CBF increased by procaterol stimulation reached a plateau within 3 min (the normalized CBFs at 2 and 3 min were 1.47 ± 0.05 ($n = 4$) and 1.67 ± 0.03 ($n = 4$), respectively), whereas in the control solution, it did not reach a plateau within 3 min but required 5 min for reaching a plateau (Fig. 1b). Unlike CBF, the time course of CBA reaching a plateau after procaterol stimulation was not affected by the switch to the EGTA solution: in both solutions, CBA reached plateaus within 3 min after procaterol stimulation (compare open circles in Fig. 1b with Fig. 1d). Figure 1e shows the ratios of CBA and CBF 2.5 min after the procaterol stimulation to the basal ones in the control- and the EGTA-solution, indicating that the procaterol-stimulated increase in CBF, but not CBA, was accelerated in its time course by switching to the EGTA-solution. The procaterol-stimulated increases in CBA and CBF were fitted to an exponential curve, $a \cdot [1 - \exp(-t/\tau)]$ (a is a constant, t is the time from the start of procaterol stimulation, and “ τ ” is the time constant), and the value of τ was used to assess the rate of CBA or CBF increase stimulated by procaterol. In Fig. 1f, the relative increases (%) in CBA and CBF and the fitted curves obtained in the EGTA solution were plotted, and also those in the control solution. The relative values were calculated as $(CBA_t - CBA_0)/(CBA_{10\text{min}} - CBA_0)$ and $(CBF_t - CBF_0)/(CBF_{10\text{min}} - CBF_0)$ (the subscript t , 0, and 10 min show the time from the start of procaterol stimulation). Upon stimulation with

procaterol, the EGTA solution shifted the CBF curve to the left, but not the CBA curve (Fig. 1f). The value of τ for CBF increase stimulated by procaterol (2.06 ± 0.18 min, $n = 4$) in the EGTA solution was smaller than that (3.61 ± 0.38 min, $n = 6$) in the control solution (significantly different, $p < 0.05$), although the values of τ for CBA increase were similar in both solutions (1.00 ± 0.21 min in the EGTA solution and 0.87 ± 0.10 min in the control solution). Thus, the EGTA-induced low $[Ca^{2+}]_i$ accelerated the procaterol-stimulated increase in CBF.

CBA and CBF increased by IBMX To accumulate cAMP without β_2 -receptor activation in the ciliary cells, we used IBMX (a nonspecific inhibitor of PDE). IBMX ($100 \mu\text{M}$), unlike the case of procaterol, increased CBA and CBF in an identical time course (Fig. 2a). CBA and CBF reached plateaus within 3 min after the IBMX addition and the ratios of CBA and CBF at 3 min were 1.69 ± 0.03 ($n = 5$) and 1.78 ± 0.08 ($n = 5$), respectively (Fig. 2a, b). Similar results were obtained by $100 \mu\text{M}$ 8-Br-cAMP (data not shown). The τ s for IBMX-stimulated CBA and CBF increase obtained by the curve fitting were 1.03 ± 0.11 and 1.28 ± 0.07 min ($n = 5$), respectively (not significantly different). The concentration-response studies of IBMX showed that the CBF curve was almost similar to the CBA curve (the EC_{50} is $5.5 \mu\text{M}$ for CBA and is $13.1 \mu\text{M}$ for CBF), unlike a case of procaterol (Fig. 2c) [15]. These observations (Figs. 1 and 2) suggest that a Ca^{2+} -dependent PDE (PDE1) affects the CBF increase stimulated by procaterol.

Effects of 8-methoxymethyl-IBMX (8MmIBMX, a selective PDE1 inhibitor) on CBA and CBF The effects of a selective inhibitor of PDE1, $40 \mu\text{M}$ 8MmIBMX, were examined. The addition of 8MmIBMX ($40 \mu\text{M}$) alone increased CBA and CBF (Fig. 3a). The normalized values of CBA and CBF at 5 min after the 8MmIBMX addition were 1.11 ± 0.01 ($n = 6$) and 1.23 ± 0.04 ($n = 6$), respectively. The further addition of procaterol increased CBA and CBF in an identical time course. Figure 3b shows the relative increases in CBA and CBF to compare the time courses between CBA and CBF increase. The τ s for the procaterol-stimulated CBA and CBF increase obtained by the curve fitting were similar, 2.81 ± 0.30 min for CBA increase and 2.54 ± 0.20 min for CBF increase ($n = 6$). The ratios of CBA and CBF 3 min after the procaterol stimulation were shown in Fig. 3c. In the presence of 8MmIBMX, both CBA and CBF plateaued within 3 min after the procaterol stimulation. The prior treatment of $1 \mu\text{M}$ PKI-A for 10 min abolished increases in CBF or CBA induced by 8MmIBMX, and it inhibited the increases in CBA and CBF stimulated by procaterol by 50% (Fig. 3d). This indicates that 8MmIBMX accumulates cAMP in the airway ciliary cells. Thus, an inhibitor of PDE1 abolished the differences in the time courses between CBA and CBF increase

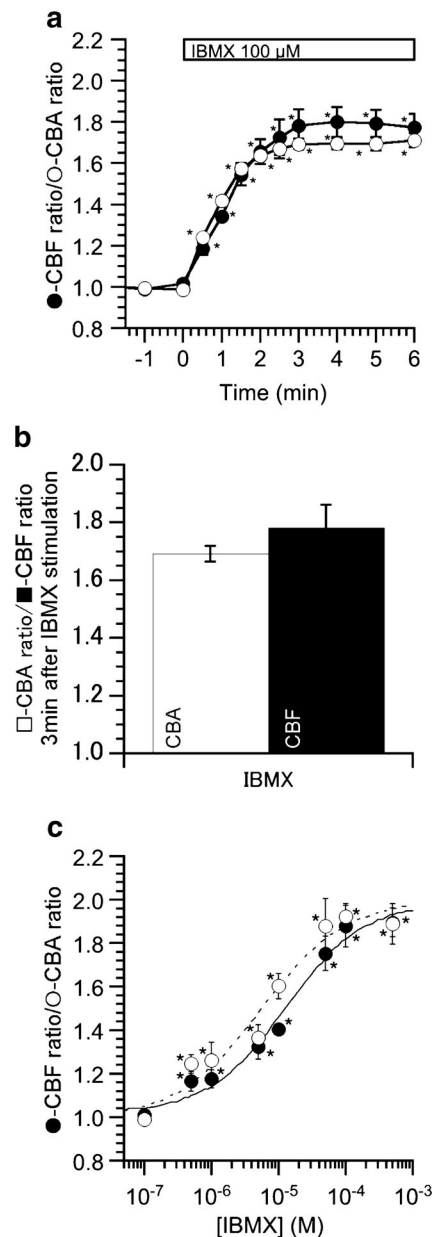


Fig. 2 Effects of IBMX on CBA and CBF. **a** IBMX ($100 \mu\text{M}$). The addition of IBMX increased both CBA and CBF in an identical time course. The *asterisk signs* indicate significantly different from the values of CBA and CBF before IBMX stimulation ($p < 0.05$). **b** The ratios of CBA and CBF at 3 min from the start of IBMX stimulation. Both CBA and CBF reached plateaus within 3 min. **c** Concentration-response study of IBMX. The IBMX concentration-response curve of CBA was similar to that of CBF. The *asterisk signs* indicate significantly different from the values of CBA and CBF stimulated with 100 nM IBMX ($p < 0.05$)

stimulated by procaterol, suggesting that PDE1 degrades cAMP in the CBF-regulating metabolon.

Effects of BAPTA-AM and calmidazolium (a calmodulin inhibitor) Since PDE1 is a Ca^{2+} /calmodulin-dependent enzyme, we examined the effects of an $[Ca^{2+}]_i$ lowered by

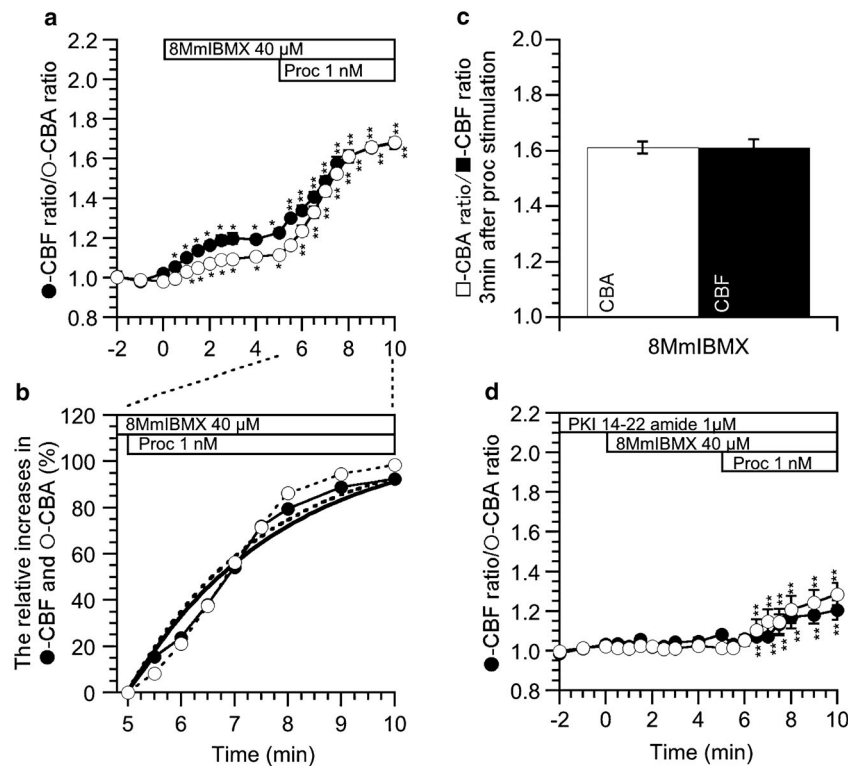


Fig. 3 Effects of 8MmIBMX (40 μM , an inhibitor of PDE1) on CBA and CBF. **a** 8MmIBMX alone increased CBF and CBA, and then, the further procaterol stimulation increased CBA and CBF in an identical time course. The *single asterisk signs* indicate significantly different from the values of CBA and CBF before 8MmIBMX stimulation ($p < 0.05$). The *double asterisk signs* indicate significantly different from the values of CBA and CBF just before the start of procaterol stimulation ($p < 0.05$). **b** The relative increase ratios of CBA and CBF in the first 5 min from the start of procaterol stimulation. In the presence of 8MmIBMX, procaterol stimulation increased CBA and CBF in an identical time course. To compare the rates of procaterol-stimulated CBA and CBF increase, the plots were fitted to the exponential curve,

as shown in Fig. 1f. The curve for the CBF increase was shown as the *solid line* and that for the CBA increase was as the *dotted line*. **c** Comparison of the ratios of CBA and CBF at 3 min from the start of 8MmIBMX stimulation. Both ratios reached plateaued within 3 min. **d** Cells were treated with PKI-A for 10 min prior to the addition of 8MmIBMX. In the presence of PKI-A, 8MmIBMX did not increase CBF and CBA. The further procaterol stimulation induced small increases in CBF or CBA. The ratios of CBA and CBF 10 min after the procaterol stimulation were 1.33 ± 0.04 ($n = 3$) and 1.28 ± 0.05 ($n = 3$), respectively. The *double asterisk signs* indicate significantly different from the values of CBA and CBF before procaterol stimulation ($p < 0.05$)

BAPTA-AM on CBA and CBF. To decrease the $[\text{Ca}^{2+}]_i$ to an extremely low level, cells were treated with a nominally Ca^{2+} -free solution containing BAPTA-AM (50 μM) (BAPTA-AM treatment). The BAPTA-AM treatment increased CBA and CBF. The normalized values of CBA and CBF at 5 min after the BAPTA-AM treatment were 1.11 ± 0.02 ($n = 4$) and 1.11 ± 0.01 ($n = 4$), respectively (Fig. 4a). The further procaterol stimulation increased CBA and CBF in an identical time course. The τ s for the procaterol-stimulated CBA and CBF increase obtained by the curve fitting were 3.30 ± 0.46 and 2.93 ± 0.64 min ($n = 4$, not significantly different). The normalized values of CBA and CBF 3 min after the procaterol stimulation were 1.31 ± 0.04 and 1.39 ± 0.11 , respectively. We also treated cells with a nominally Ca^{2+} -free solution containing 5 and 25 μM BAPTA-AM. However, at concentrations less than 25 μM , BAPTA-AM did not induce any changes in CBA and CBF as shown in the previous report [17].

The experiments were also carried out using calmidazolium (25 μM , a calmodulin inhibitor).

Calmidazolium at 25 μM increased CBA and CBF (Fig. 4b), similarly to the 50 μM BAPTA-AM (Fig. 4a). The normalized CBA and CBF 5 min after the calmidazolium addition were 1.12 ± 0.01 ($n = 4$) and 1.14 ± 0.02 ($n = 4$), respectively. The further procaterol stimulation increased CBA and CBF in an identical time course. The τ s for the procaterol-stimulated CBA and CBF increase obtained by the curve fitting were 3.16 ± 0.23 and 3.00 ± 0.59 min ($n = 4$, not significantly different). The normalized CBA and CBF 3 min after the procaterol stimulation were 1.34 ± 0.05 and 1.37 ± 0.05 , respectively. We also examined the effects of 5 μM calmidazolium on CBA and CBF. Calmidazolium at 5 μM induced no change in CBA and a slight decrease in CBF (0.5–1 Hz). Similar observations using 1 μM calmidazolium have been shown in a previous report [22]. The ratios of CBA and CBF 3 min after the procaterol stimulation are shown in Fig. 4c. In the presence of BAPTA-AM or calmidazolium, CBA and CBF stimulated by procaterol plateaued within 5 min. Thus, BAPTA-AM or calmidazolium

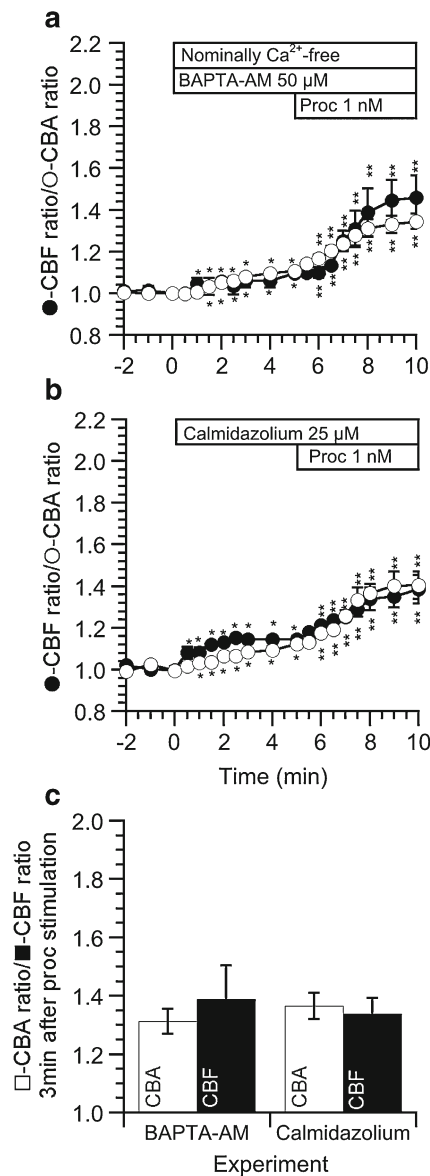


Fig. 4 Effects of BAPTA-AM and calmidazolium on CBA and CBF. **a** BAPTA-AM (50 μM). The switch to the nominally Ca²⁺-free solution containing 50 μM BAPTA-AM increased both CBA and CBF. The further procaterol stimulation increased CBA and CBF in an identical time course. **b** Calmidazolium (25 μM, a calmodulin inhibitor). The addition of calmidazolium increased both CBA and CBF. The further procaterol stimulation increased CBA and CBF in an identical time course. **c** Comparison of the ratios of CBA and CBF at 3 min from the start of procaterol stimulation in cells treated with BAPTA-AM or with calmidazolium. The ratios of CBA and CBF stimulated by procaterol in cells treated with BAPTA-AM were replotted from the **a** and those treated with calmidazolium were replotted from the **b**. Both ratios reached plateaued within 3 min. The *single asterisk signs* indicate significantly different from the values of CBA and CBF before the calmidazolium addition ($p < 0.05$). The *double asterisk signs* indicate significantly different from the values of CBA and CBF before procaterol stimulation ($p < 0.05$)

mimicked the effects of 8MmIBMX on CBA and CBF in lung airway ciliary cells.

cAMP contents in the isolated lung cells The cAMP contents of the isolated lung cells were measured (Fig. 5). The cells were treated with test solutions for 15 min. In the vehicle control (DMSO) experiment, the cAMP content of the isolated lung cells was 17.4 ± 0.6 μmoles/g-protein ($n = 3$). The cAMP contents (μmoles/g-protein) were 23.0 ± 1.6 ($n = 3$) in the cells treated with the EGTA solution, 26.1 ± 1.3 ($n = 3$) with the nominally Ca²⁺ solution containing 50 μM BAPTA-AM, 27.2 ± 1.1 ($n = 3$) with 8MmIBMX, 26.3 ± 1.3 ($n = 3$) with calmidazolium, 22.1 ± 2.0 ($n = 3$) with procaterol, 163.1 ± 4.5 ($n = 3$) with IBMX, and 198.2 ± 6.3 ($n = 3$) with procaterol plus IBMX. The amount of cAMP increase stimulated by procaterol for 15 min was similar to those stimulated by other drugs except IBMX, while the extents of CBA and CBF increase stimulated by procaterol were much greater than those stimulated by other drugs. Moreover, IBMX increased cAMP contents much greater than other drugs. Since some parts of cAMP produced by procaterol stimulation may be broken down by PDE, the cAMP contents at an earlier time, such as 3 min, after procaterol stimulation were measured. The cAMP content of the cells treated with procaterol for 3 min was 27.6 ± 1.7 μmoles/g-protein ($n = 3$), which was larger than that after the 15-min treatment of procaterol ($p < 0.05$). Increases in the cAMP contents stimulated by procaterol are transient.

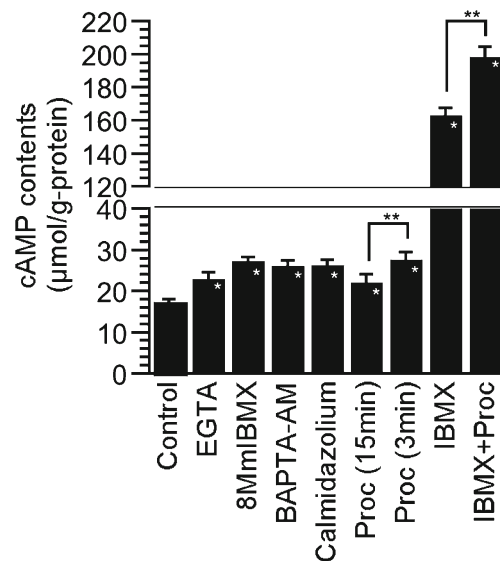


Fig. 5 The cAMP contents of isolated lung cells. The isolated lung cells were incubated with the EGTA solution, 8MmIBMX, BAPTA-AM, calmidazolium, procaterol, IBMX, and IBMX plus procaterol for 15 min. 8MmIBMX, BAPTA-AM, calmidazolium, and procaterol increased cAMP contents of isolated lung cells to 130–150%. Upon stimulating with procaterol, the cAMP contents for 3-min stimulation were greater than those for 15-min stimulation. However, IBMX increased cAMP contents 10 times greater than that of control, and in the presence of IBMX, procaterol stimulation further increased cAMP contents. The *single asterisk signs* indicate significantly different from the control ($p < 0.05$). The *double asterisk signs* indicate significantly different ($p < 0.05$)

Measurement of $[Ca^{2+}]_i$ in the isolated ciliary cells We measured the $[Ca^{2+}]_i$ using a Ca^{2+} -sensitive fluorescence dye, fluo 4. The switch to the EGTA solution from the control solution immediately decreased the fluo 4 fluorescence ratio (F/F_0) (F/F_0 5 min after the switch = 0.57 ± 0.02 , $n = 3$). Then, we switched to the BAPTA-AM (50 μ M)-containing nominally Ca^{2+} -free solution (second switch). The second switch further decreased F/F_0 (F/F_0 10 min after the second switch = 0.41 ± 0.02) (Fig. 6). Thus, the addition of 50 μ M BAPTA-AM further decreased the $[Ca^{2+}]_i$ from that decreased by the EGTA solution.

Expression of PDE1 in the lung airway cilia The Western blot analysis for PDE1 (PDE1A, PDE1B, and PDE1C) were carried out using the isolated lung cells and brain. In the isolated lung cells, the bands for PDE1A (65 kDa) and for PDE1C (70 kDa) were detected, but not that for PDE1B (60 kDa) (Fig. 7).

The PDE1 localization in the cilium was examined by the immunoelectron microscopy. In the immunoelectron micrographs, the immuno-gold particles labeled by PDE1A were detected in the airway cilia (Fig. 8a, b), but not those labeled by PDE1B (Fig. 8d), PDE1C (Fig. 8e), and Rabbit IgG (Fig. 8f). A conventional electron micrograph using epoxy resin section (Fig. 8c) clearly shows the axonemal structure (9 + 2 structure). A cilium observed by the conventional electron micrograph was shown in Fig. 8(C2) and that by the immunoelectron micrograph was shown in Fig. 8(C3), and the cell membrane (marked by black arrows) and the

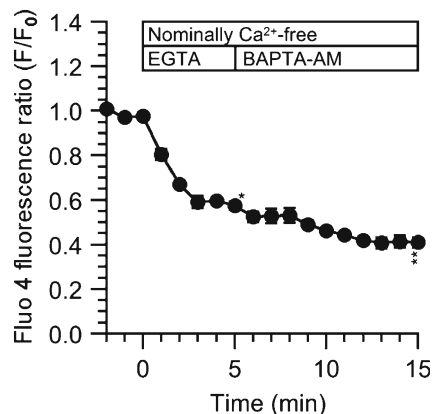


Fig. 6 Changes in the $[Ca^{2+}]_i$ in the EGTA solution and in the BAPTA-AM containing Ca^{2+} -free solution. $[Ca^{2+}]_i$ were monitored by using Ca^{2+} -sensitive fluorescence dye (fluo 4, Ex 488 nm, Em 510 nm) in lung airway ciliary cells. Changes in the $[Ca^{2+}]_i$ were expressed by the ratio of fluo 4 fluorescence (F/F_0). The subscript t and 0 show the time from the start of experiments. The switch to the EGTA solution immediately decreased F/F_0 and then, the switch to the BAPTA-AM containing Ca^{2+} -free solution further decreased it. The *single asterisk signs* indicate significantly different from the values F/F_0 before switch to the EGTA solution. ($p < 0.05$). The *double asterisk signs* indicate significantly different from the values F/F_0 before the switch to the BAPTA-AM containing Ca^{2+} -free solution ($p < 0.05$)

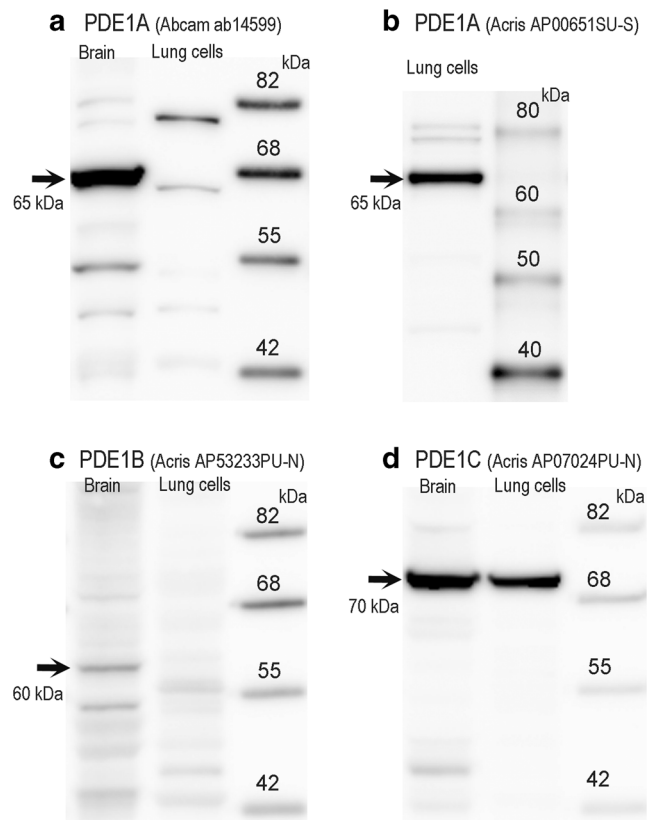
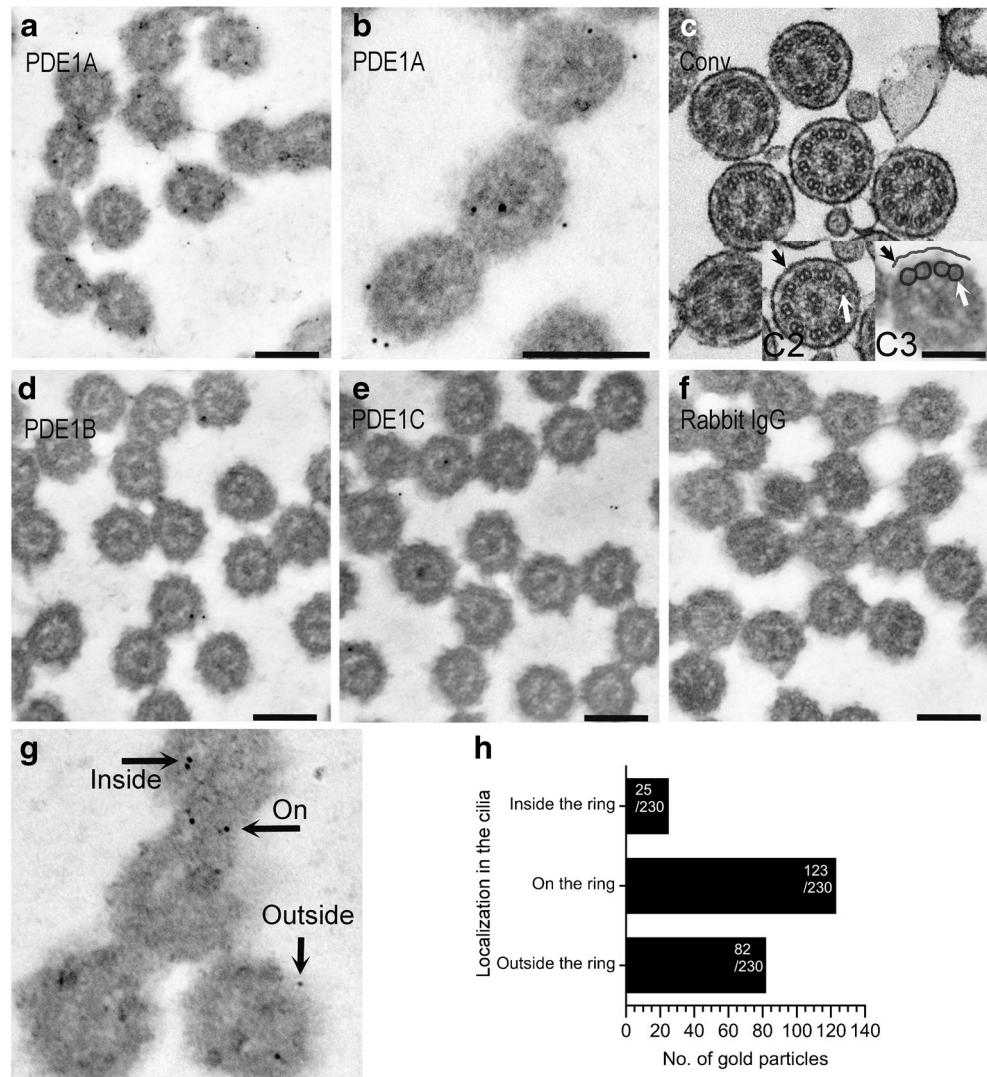


Fig. 7 Western blotting for PDE1A, PDE1B, and PDE1C of the isolated lung cells. The bands for PDE1A and PDE1C were detected in the isolated lung cells. But no band for PDE1B was noted

comparison of panels C2 with C3 enabled us to detect nine doublet tubules (marked by white arrows) in a cilium of the immunoelectron micrograph. The immuno-gold particles labeling PDE1A were preferentially found on the nine doublet tubules ring and outside the ring in the cilia (Fig. 8a, b). A small number of the immuno-gold particles were found inside of the nine doublet tubules ring. We counted the number of immuno-gold particles labeling PDE1A inside the ring, on the ring, and outside the ring in the cilia (Fig. 8g), using 10 immunoelectron micrographs. The numbers of immuno-gold particles labeling PDE1A inside the ring, on the ring, and outside the ring in the cilia were 25, 132, and 82, respectively (Fig. 8h). Most of immuno-gold particles labeling PDE1A were detected on the ring and outside the ring in the cilium. The immuno-gold particles labeling PDE1A were also found in the cell body, especially in the mitochondria. The immuno-gold articles labeled by PDE1C were not found in the cilia (Fig. 8e) but they were in the cell body, especially in the mitochondria (data not shown). Thus, in the lung airway ciliary cells, PDE1A exists on the nine doublet tubules ring and outside the ring in the cilia.

Similar results were obtained by the immunofluorescence examinations for PDE1A, PDE1B, and PDE1C using isolated lung airway ciliary cells (data not shown).

Fig. 8 Localization of PDE1A in the cilia detected by an immunoelectron microscopy. **a** PDE1A. Low magnification. **b** PDE1A. High magnification. Immuno-gold particles were detected on the nine doublet tubules ring and the outside of axoneme in the cilium. **c** Conventional electron micrograph of bronchiolar cilia. A cilium observed by the conventional electron microscopy (C2) and a cilium observed by the immunoelectron microscopy (C3). The *black arrows* show the cell membranes and the *white arrows* show the nine doublet tubules ring. **d** PDE1B and **e** PDE1C. Few immuno-gold particles for PDE1B (**d**) and PDE1C (**e**) were detected in the cilia. **f** Non-immunized rabbit IgG. No immuno-gold particles were detected in the cilia. **g** and **h**: Localization of gold particles in the cilia. The immuno-gold particles located inside the ring, on the ring and outside the ring in the cilia were shown in **g**. The immuno-gold particles were counted using 10 immunoelectron micrographs. Most of gold particles were detected on the ring and outside of the axoneme in the cilium. Scale bar, 200 nm



Discussion

This study demonstrates that Ca^{2+} /calmodulin-dependent PDE1A exists in the CBF-regulating metabolon (the nine doublet tubules and outside of the nine doublet tubules), not in the CBA-regulating metabolon (inside of the nine doublet tubules) of lung airway cilia. The PDE1A degrades cAMP accumulated in the CBF-regulating metabolon. The previous study showed that procaterol increases CBA and CBF via cAMP accumulation, but that the time course of CBF increase was slower than that of CBA increase [15]. However, it remained uncertain why the time course of CBF increase was slower than that of the CBA increase. The results of this study indicate that the time course of cAMP accumulation stimulated by procaterol is slower in the CBF-regulating metabolon than in the CBA-regulating metabolon, and that the slower cAMP accumulation in the CBF-regulating metabolon causes a slower increase in CBF than that in CBA.

PDE1A is a Ca^{2+} /calmodulin-dependent enzyme [2, 8]. The present study demonstrated that an $[\text{Ca}^{2+}]_i$ lowered by the EGTA solution increased the rate of CBF increase stimulated by procaterol compared with that maintained by the control solution, but not the rate of CBA increase. Moreover, calmodulin inhibited by an extremely low $[\text{Ca}^{2+}]_i$ (50 μM BAPTA-AM in a Ca^{2+} -free solution) or by 25 μM calmidazolium increased CBF, similarly to 8mM IBMX (a selective PDE1 inhibitor). These results suggest that the Ca^{2+} /calmodulin-dependent PDE1A regulates CBF of the lung airway cilia. However, a previous study showed that a low concentration of calmidazolium, such as 1 μM , decreased CBF by 1 Hz from the baseline CBF [22]. In this study, calmidazolium at concentrations less than 5 μM also decreased CBF by 0.5–1 Hz (data not shown) from the baseline CBF (10–12 Hz). Moreover, a low concentration of BAPTA-AM, such as 10 μM , has shown to have no effect on the baseline CBF [17]. In this study, BAPTA-AM at concentrations less than

25 μM also did not change the baseline CBF. These observations indicate that a high concentration of calmidazolium, such as 25 μM , or an extremely low $[\text{Ca}^{2+}]_i$ is required for the complete inhibition of calmodulin, which inhibits PDE1 in the lung airway ciliary cells.

On the other hand, in the presence of BAPTA-AM (50 μM) or calmidazolium (25 μM), procaterol increases CBA and CBF, but the extents of CBA and CBF increase are smaller than those in the absence of BAPTA-AM or calmidazolium. One possible explanation is that an extremely low $[\text{Ca}^{2+}]_i$ or inhibition of calmodulin may decrease the cAMP production, because the bronchial epithelia express the isoforms of Ca^{2+} -dependent adenylyl cyclase (type III and type VIII) [14]. A decrease in cAMP production appears to decrease the extents of the procaterol-stimulated CBA and CBF increase.

A high concentration of calmidazolium (10 μM) has reported to be toxic in ovine tracheal ciliary cells [22]. In this study, calmidazolium at 50 μM gradually decreased CBA and CBF to 20–30% and it stopped the ciliary beating in some ciliary cells (approximately 30% cells) (data not shown). However, 25 μM calmidazolium or 50 μM BAPTA-AM increased the baseline CBA and CBF and procaterol still increased CBA and CBF. These observations suggest that the toxic effects of calmidazolium and BAPTA-AM would be negligibly small in our experimental condition, although we could not neglect their toxic effects.

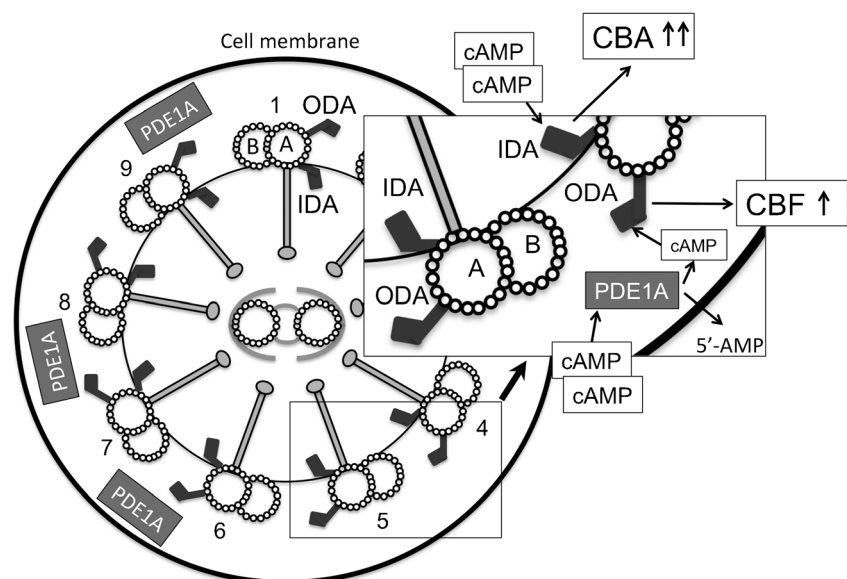
In the present study, the PDE1A exists in the cilia and the cell body of lung airway ciliary cells, but PDE1C exists only in the cell body of the ciliary cells, but not in the cilia. Similar findings have shown in the sperm [16, 27]. The roles of PDE1A and PDE1C in the sperm still remain uncertain, although PDE1A and PDE1C are thought to control the ciliary beating and the flagella beating involving an interplay

between cAMP and Ca^{2+} signal [16, 27]. In the lung airway cilia, PDE1A appears to play a role for maintaining an adequate CBF by degrading cAMP excessively accumulated. The adequate CBF may be beneficial for energy supply and consumption of the lung airway ciliary cells. Further studies are required to understand the role of PDE1A and PDE1C for the airway ciliary beating.

An inhibition of PDE1 by 8MmIBMX, BAPTA-AM, or calmidazolium increased not only CBF but also CBA. The CBA increase evoked by an inhibition of PDE1 is induced by cAMP accumulation, because it is inhibited by PKI-A (an inhibitor of PKA). 8MmIBMX, BAPTA-AM, or calmidazolium stimulates cAMP accumulation in the cell body by inhibiting two subtypes of PDE1 (PDE1A and PDE1C) and modulates it in the CBF-regulating metabolon by inhibiting PDE1A leading to the CBF increase, although the cAMP accumulation stimulated by the inhibition of PDE1A and PDE1C also increases CBA.

In the presence of IBMX, procaterol accumulates much larger amount of cAMP ($\Delta\text{cAMP} = 35 \mu\text{moles/g-proten}$ for 15 min), compared with that in the absence of IBMX ($\Delta\text{cAMP} = 4.7 \mu\text{moles/g-proten}$ for 15 min). Moreover, IBMX alone accumulated a large amount of cAMP. These indicate that a large amount of cAMP is produced in the lung airway ciliary cells and is degraded by PDE. At present, we do not know the molecular mechanism for the regulation of cAMP production in unstimulated lung airway ciliary cells. However, it is certain that the turnover of cAMP is rapid in unstimulated lung airway ciliary cells. The addition of PKI-amide alone decreased CBA and CBF by approximately 10% (data not shown) even under the unstimulated condition. This suggests that the maintenance of an adequate cAMP concentration in the cilia is essential for keeping adequate CBA and CBF.

Fig. 9 Regulation of CBF and CBA in the lung airway ciliary cell during procaterol stimulation



Previous studies have shown to exist PDE 3, 4, 5, and 7 in the human airway epithelial cells, in addition to PDE1 [9, 26], and their inhibitors elevate the cAMP contents [9] and to increase CBF in the airway ciliary cells [26, 30]. In their reports, the inhibition of PDE4 accumulates a large amount of cAMP compared with the inhibition of other PDE subtypes [9]. Our preliminary study indicated that rolipram (10 μ M, an inhibitor of PDE4) increased CBA and CBF by 30% and the time course of CBF increase was slower than that of CBA increase. The values of τ were 2.15 ± 0.21 min ($n = 5$) for the CBA increase and 4.00 ± 0.63 min ($n = 5$) for the CBF increase. The results indicate that PDE4 also degrades cAMP in the lung airway ciliary cells, in addition to PDE1. PDE4 plays an important role in the maintenance of an adequate cAMP level in lung airway ciliary cells, although at present, we have no data on other PDE subtypes (PDE3, 5, 7).

Moreover, the cAMP contents produced by procaterol were much less, compared with those expected from the CBA and CBF increase. However, the IBMX experiments indicate that a large amount of cAMP was produced by the procaterol stimulation. A high cAMP concentration, such as 100 μ M, is required to increase CBA and CBF as shown in the experiments of 8BrcAMP. A possible explanation is that the cAMP concentration in the cilia is higher than that of the cell body. This study demonstrated that PDE1C exists in the cell body, but not in the cilia. Some subtypes of PDE, such as PDE4 [9, 26], may also exist only in the cell body, not in the cilia, of lung airway ciliary cells, although we do not know the subcellular localization of PDE4 at present. Moreover, an increase in the cAMP concentration stimulated by procaterol is transient in these cells when we measure the average of the cAMP contents in the overall areas of intracellular spaces but not the cAMP content in the special area such as the ciliary area. This may also induce large increases in CBA and CBF in the lung airway ciliary cells during procaterol stimulation even if we observed only a small increase in the average of cAMP concentration in overall intracellular spaces. Namely, procaterol might induce large elevation of cAMP concentration on the ciliary area even if the procaterol-induced average increase in the cAMP concentration in the overall intracellular space would be small, and this large elevation of cAMP concentration in the ciliary area would increase CBA and CBF. To confirm this point, further experiments are required.

Airway ciliary beating is affected by sex hormones [13], similarly to the ciliary cells of the Fallopian tube [19]. A progesterone treatment for 6 or 12 h reversibly decreases airway CBF by 30 or by 40%, respectively, while an estrogen treatment little affects it [13]. We removed the lungs from the mice 12 h after reaching the peak value in the progesterone level (the lungs were removed from the mice at \sim 10 A.M.) even on the day of ovulation (the mouse ovarian cycle is 4 days) [5]. We noted little difference in basal CBF and CBA and in the procaterol responses in CBA and CBF among mice used for

the experiments. The effects of sex hormones on the lung airway ciliary beating appear to be negligibly small in this study.

The conclusion of this study is summarized in Fig. 9. PDE1A exists outside the axoneme (on the nine doublet tubules ring and outside the ring) in the cilium. Procaterol accumulates cAMP in the lung airway ciliary cells. Accumulated cAMPs in the cell body are transported from the basal portion to the tip of cilia, and then, they activate the IDAs leading to an immediate increase in CBA via a PKA-dependent pathway. However, PDE1A exists in the CBF-regulating metabolon where ODAs function, and it degrades cAMP, leading to a slower cAMP accumulation in the ODA-regulating metabolon compared with in the IDA-regulating metabolon. Therefore, a slower cAMP accumulation in the ODA-regulating metabolon results in a slower CBF increase in the time course, compared with a CBA increase.

Acknowledgements We thank the Osaka Medical College for giving us an opportunity to perform the experiments using the video microscope equipped with a high-speed camera. This work is partly supported by the contracted research fund from Otsuka Pharmaceutical Co., Ltd. (Tokyo, Japan).

Compliance with ethical standards The procedures and protocols for the experiments were approved by the Committee for Animal Research of Kyoto Prefectural University of Medicine.

References

1. Afzelius BA (2004) Cilia-related diseases. *J Pathol* 204:470–477
2. Bender AT, Beavo JA (2006) Cyclic nucleotide phosphodiesterases: molecular regulation to clinical use. *Pharmacol Rev* 58:488–520
3. Brokaw CJ (1994) Control of flagellar bending: a new agenda based on dynein diversity. *Cell Motil Cytoskeleton* 28:199–204
4. Brokaw CJ, Kamiya R (1987) Bending patterns of *Chlamydomonas* flagella: IV. Mutants with defects in inner and outer dynein arms indicate differences in dynein arm function. *Cell Motil Cytoskeleton* 8:68–75
5. Butcher RL, Collins WE, Fugo NW (1974) Plasma concentration of LH, FSH, prolactin, progesterone and estradiol-17 β throughout the 4-day estrous cycle of the rat. *Endocrinology* 94:1704–1708
6. Chilvers MA, Rutman A, O'Callaghan C (2003) Ciliary beat pattern is associated with specific ultrastructural defects in primary ciliary dyskinesia. *J Allergy Clin Immunol* 112:518–524
7. Delmotte P, Sanderson MJ (2006) Ciliary beat frequency is maintained at maximal rate in the small airways of mouse lung slices. *Am J Respir Cell Mol Biol* 35:110–117
8. Francis SH, Blount MA, Corbin JD (2011) Mammalian cyclic nucleotide phosphodiesterase: molecular mechanism and physiological functions. *Physiol Rev* 91:651–690
9. Fuhrmann M, Jahn H-U, Seybold J, Neurohr C, Barnes PJ, Hippenstiel S, Kraemer HJ, Suttrop N (1999) Identification and function of cyclic nucleotide phosphodiesterase isoenzymes in airway epithelial cells. *Am J Respir Cell Mol Biol* 20:292–302
10. Gibbons IR, Rowe AJ (1965) Dynein: a protein with adenosine triphosphatase activity from cilia. *Science* 149:424–426
11. Hard R, Blaustein K, Scarcello L (1992) Reactivation of outer arm-depleted lung axonemes: evidence for functional differences

- between inner and outer dynein arms in situ. *Cell Motil Cytoskeleton* 21:199–209
12. Hayashi T, Kawakami M, Sasaki S, Katsumata T, Mori H, Yoshida H, Nakahari T (2005) ATP regulation of ciliary beat frequency in rat tracheal and distal airway epithelium. *Exp Physiol* 90:535–544
 13. Jain R, Ray JM, Pan J-H, Brody SL (2012) Sex hormone-dependent regulation of cilia beat frequency in airway epithelium. *Am J Respir Cell Mol Biol* 46:446–453
 14. Jourdan KB, Mason NA, Long L, Philips PG, Wilkins MR, Morrell NW (2001) Characterization of adenylyl cyclase isoforms in rat peripheral pulmonary arteries. *Am J Physiol Lung Cell Mol Physiol* 280:L1359–L1369
 15. Komatani-Tamiya N, Daikoku E, Takemura Y, Shimamoto C, Nakano T, Iwasaki Y, Kohda Y, Matsumura H, Marunaka Y, Nakahari T (2012) Procatenol-stimulated increases in ciliary bend amplitude and ciliary beat frequency in mouse bronchioles. *Cell Physiol Biochem* 29:511–522
 16. Lefèvre L, de Lamirande E, Gagnon C (2002) Presence of cyclic nucleotide phosphodiesterases PDE1A, existing as a stable complex with calmodulin, and PDE3A in human spermatozoa. *Biol Reprod* 67:423–430
 17. Li W-E, Chen W, Ma Y-F, Tuo Q-R, Luo X-J, Zhang T, Sai W-B, Liu J, Shen J, Liu Z-G, Zhen Y-M, Wang Y-X, Ji G, Liu Q-H (2012) Methods to measure and analyze ciliary beat activity: Ca²⁺ influx-mediated cilia mechanosensitivity. *Pflugers Arch Eur J Physiol* 464: 671–680
 18. Matsuzaki Y, Wu H, Nakano T, Nakahari T, Sano K (2015) ATP-association to intrabacterial nanotransportation system in *Vibrio cholerae*. *Med Mol Morphol* 48:225–234
 19. Nakahari T, Nishimura A, Shimamoto C, Sakai A, Kuwabara H, Nakano T, Tanaka S, Kohda Y, Matsumura H, Mori H (2011) The regulation of ciliary beat frequency by ovarian steroids in the guinea pig Fallopian tube: interactions between oestradiol and progesterone. *Biomed Res-Tokyo* 32:321–328
 20. Nakano T, Aoki H, Wu H, Fujioka Y, Nakazawa E, Sano K (2012) Fine visualization of filamentous structures in the bacterial cytoplasm. *J Microbiol Methods* 90:60–64
 21. Salathe M (2007) Regulation of mammalian ciliary beating. *Annu Rev Physiol* 69:401–422
 22. Salathe M, Bookman RJ (1999) Mode of Ca²⁺ action on ciliary beat frequency in single ovine airway epithelial cells. *J Physiol* 520:851–861
 23. Shiima-Kinoshita C, Min K-Y, Hanafusa T, Mori H, Nakahari T (2004) β_2 -adrenergic regulation of ciliary beat frequency in rat bronchiolar epithelium: potentiation by isosmotic cell shrinkage. *J Physiol* 554:403–416
 24. Smith RP, Shellard R, Dhillon DP, Winter J, Mehta A (1996) Asymmetric interactions between phosphorylation pathways regulating ciliary beat frequency in human nasal respiratory epithelium in vitro. *J Physiol* 496:883–889
 25. Tanaka S, Hosogi S, Sawabe Y, Shimamoto C, Matsumura H, Inui T, Marunaka Y, Nakahari T (2016) PPAR α induced NOS1 phosphorylation via PI3K/Akt in guinea pig antral mucous cells: NO-enhancement in Ca²⁺-regulated exocytosis. *Biomed Res-Tokyo* 37(3):167–178
 26. Turner MJ, Matthes E, Billet A, Ferguson AJ, Thomas DY, Randell SH, Ostrowski LE, Abbott-Banner K, Hanrahan JW (2016) The dual phosphodiesterase 3 and 4 inhibitor RPL554 stimulates CFTR and ciliary beating in primary cultures of bronchial epithelia. *Am J Physiol Lung Cell Mol Physiol* 310:L59–L70
 27. Vasta V, Sonnenburg WK, Yan C, Soderling SH, Shimizu-Albergine M, Beavo JA (2005) Identification of a new valiant of PDE1A calmodulin-stimulated cyclic nucleotide phosphodiesterase expressed in mouse sperm. *Biol Reprod* 73:598–609
 28. Wanner A, Salathe M, O’riordan TG (1996) Mucociliary clearance in the airways. *Am J Respir Crit Care Med* 154:1968–1902
 29. Wood CR, Hard R, Hennessey TM (2007) Targeted gene disruption of dynein heavy chain 7 of *Tetrahymena thermophila* results in altered ciliary waveform and reduced swim speed. *J Cell Sci* 120: 3075–3085
 30. Wyatt TA, Forgèt MA, Sisson JH (2003) Ethanol stimulates ciliary beating by dual cyclic nucleotide kinase activation in bovine bronchial epithelial cells. *Am J Pathol* 163:1157–1166